Ersch. in: Crystallisation - a biological perspective; University of Leeds, UK, 23-25 July 2012 / ed. Philip Earis. - Cambridge : RSC Publ. - S. 291-312. - (Faraday discussions ; 159). - ISBN 978-1-84973-450-9

http://dx.doi.org/10.1039/C2FD20080E

A metastable liquid precursor phase of calcium carbonate and its interactions with polyaspartate

Mark A. Bewernitz,[a] Denis Gebauer,[b] Joanna Long,[c] Helmut Cölfen[d] and Laurie B. Gower*[e]

Invertebrate organisms that use calcium carbonate extensively in the formation of their hard tissues have the ability to deposit biominerals with control over crystal size, shape, orientation, phase, texture, and location. It has been proposed by our group that charged polyelectrolytes, like acidic proteins, may be employed by organisms to direct crystal growth through an intermediate liquid phase in a process called the polymer induced liquid precursor (PILP) process. Recently, it has been proposed that calcium carbonate crystallization, even in the absence of any additives, follows a non classical, multi step crystallization process by first associating into a liquid precursor phase before transition into solid amorphous calcium carbonate (ACC) and eventually crystalline calcium carbonates. In order to determine if the PILP process involves the promotion, or stabilization, of a naturally occurring liquid precursor to ACC, we have analyzed the formation of saturated and supersaturated calcium carbonate bicarbonate solutions using Ca^{2+} ion selective electrodes, pH electrodes, isothermal titration calorimetry, nanoparticle tracking analysis, ^{13}C T_2 relaxation measurements, and ^{13}C PFG STE diffusion NMR measurements. These studies provide evidence that, in the absences of additives, and at near neutral pH (emulating the conditions of biomineralization and biomimetic model systems), a condensed phase of liquid like droplets of calcium carbonate forms at a critical concentration, where it is stabilized intrinsically by bicarbonate ions. In experiments with polymer additive, the data suggests that the polymer is kinetically stabilizing this liquid condensed phase in a distinct and pronounced fashion during the so called PILP process. Verification of this precursor phase and the stabilization that polymer additives provide during the PILP process sheds new light on the mechanism through which biological organisms can exercise such control over deposited $CaCO_3$ biominerals, and on the potential means to generate *in vitro* mineral products with features that resemble biominerals seen in nature.

[a]*Department of Biomedical Engineering, University of Florida, Gainesville, FL, 32611 64000, USA. E mail: bewerni1@ufl.edu; Tel: +1 352 846 3337*

[b]*Department of Chemistry, Physical Chemistry, University of Konstanz, Universitatsstrasse 10, Box 714, D 78457 Konstanz, Germany. E mail: Denis.Gebauer@uni konstanz.dez; Fax: +49 7531 883139; Tel: +49 7531 882169*

[c]*Department of Biochemistry and Molecular Biology, University of Florida, Gainesville, FL, USA*

[d]*Department of Chemistry, Physical Chemistry, University of Konstanz, Universitatsstrasse 10, D 78457 Konstanz, Germany. E mail: Helmut.Coelfen@uni konstanz.de; Fax: +49 7531 883139; Tel: +49 7531 884063*

[e]*Department of Materials Science and Engineering, University of Florida, Gainesville, FL, 32611 6400, USA. E mail: lgowe@mse.ufl.edu; Tel: +1 352 846 3336*

Introduction

Calcium carbonate is one of the most abundant biominerals on Earth.[1–4] Calcium carbonate is very important in many industrial processes such as in fillers for paper making and other composites, in carbon dioxide storage for environmental concerns,[5] and in biomedical applications, such as drug delivery,[6] due to its low cost and biocompatibility.[7] From an engineering standpoint, understanding the biological formation and regulation of calcium carbonate biominerals is very intriguing because biologically derived calcium carbonate exhibits an incredible array of crystals with complex and non faceted morphologies. In nature, it is usually found as the mineral component in skeletal structures in invertebrates, such as in the spine of sea urchins[8] and in the nacre of molluscs, but plays a role in the otoliths and bones of vertebrates as well.[9,10] The additional control over mineral product displayed by biological organisms, as opposed to *in vitro* techniques, is believed to be due to cellular manipulation of an amorphous calcium carbonate (ACC) precursor phase which may act as a reactive intermediate in generating complex functional materials.[11,12] This may be due to the fact that ACC is not subject to constraints of crystal lattice energies and can be "moulded" into an endless array of non equilibrium morphologies.[3]

Manipulation of the ACC precursor may be achieved by templating and altering environmental influences to direct the formation of crystalline calcium carbonate product, which may be calcite, aragonite, and even vaterite [13] (although the latter case often serves as a crystalline intermediate).[14–16] It has been demonstrated with *in vitro* model systems that the crystalline morphology can be directed by the presence of negatively charged polyelectrolytes (that are believed to emulate the acidic proteins of biominerals) during the precipitation process, such as is proposed by the polymer induced liquid precursor (PILP) process, where a pseudomorphic transformation of a fluidic ACC precursor can lead to crystals with non equilibrium morphologies.[17,18]

During the PILP process, $CaCO_3$ appears to nucleate through a multistep step process where the polymer (charged, anionic polyelectrolyte) associates with Ca^{2+} and CO_3^{2} ions to form an intermediate liquid phase prior to solid nucleation. This is why the PILP process is so successful in generating "molten" morphologies and films because the precursor nanodroplets are believed to meld together to form smooth mineral products that lack the facets found in crystals grown by the classical crystallization process. It is difficult, however, to theoretically explain how a true liquid metastable phase can be induced by the presence of a polymer while assuming that, in the absence of polymer additives, the nucleation follows the classical view of crystallization.

According to the classical view, the formation of $CaCO_3$ nucleation proceeds *via* a nucleation and growth mechanism where the basic constituents of the crystal (ions, molecules, or atoms, depending on the material) remain soluble until a critical concentration is achieved, allowing for a critical nucleus to be formed. Recently, it has been found that $CaCO_3$ nucleation occurs through a non classical process, where a stable prenucleation solute interaction, called a prenucleation cluster (PNC) forms. The PNC formation has been reported at pHs ranging from 9.0 to 10.0 and has been reported to be stable with respect to the initial ions in solution, prior to the formation of a metastable solid nucleus of ACC.[19] Gebauer *et al.* demonstrated that Ca^{2+} and CO_3^{2} ions associate into clusters of ions (having a typical diameter on the order of *ca.* 2 3 nm) in undersaturated, saturated and supersaturated conditions.[20] The presence of PNCs has been corroborated by cryo TEM experiments in solutions saturated with respect to calcite.[21] Evidence has been obtained in the form of computer simulations that suggest that $CaCO_3$ PNCs form as stable, rapidly exchanging, branched "polymers" of alternating Ca^{2+} and CO_3^{2} ions.[22] This dynamically ordered liquid like oxyanion polymer (DOLLOP) model

for the formation of PNCs proposed by Gale *et al.* further supports the notion that PNCs are non classical by nature.

Other studies have shown evidence of a multi step model in addition to that of the PNCs proposed by Gebauer, where amorphous calcium carbonate might be formed through a liquid liquid phase separation from the bulk solution in the form of drop lets. It has been proposed for some time now that a liquid liquid phase transition might be induced by the presence of additives, such as polymers, to form droplets that can grow from tens of nanometres to as large as microns in diameter.[17] However, there has been considerable evidence recently that $CaCO_3$ transitions through very large liquid precursor droplets in the absence of any additives.[23 25] By analyzing an acoustically levitated droplet of saturated $CaCO_3$ (with respect to calcite) at a pH of 6.3, Wolf *et al.*[25] demonstrated that a liquid phase of $CaCO_3$ precursor droplets forms in supersaturated conditions, which arises from an increase in pH upon outgassing of CO_2. The liquid precursor phase was observed to form with droplet diameters of up to several hundred nanometres. Rieger *et al.*[23] quenched and freeze captured a solution after inducing precipitation by rapidly mixing Ca Cl_2(aq) and Na_2CO_3(aq) (presumably at a pH in the upper 10s) and used cryo TEM to visualize droplets of $CaCO_3$ precursor up to 2 μm in diameter. Faatz *et al.*[24] used a CO_2 outgassing technique at pH 7 to demonstrate that ACC with diameters of hundreds of nm can be obtained through a suspected liquid liquid phase separation prior to solidification into the amorphous state. Evidence of multi step mechanisms is not limited only to $CaCO_3$ mineralization, but can occur in other metal carbonates,[24 27] in calcium oxalate systems[28] phosphate coordinated systems,[29 33] as well as in organics, such as biopolymers,[34,35] amino acids[36 39] and organic pigments.[40]

In these previous works by Wolf, Rieger, and Faatz, the detected liquid precursor droplets in their experiments suggests that the liquid phase is metastable with respect to the phases that occur at later stages, and that the structural transitions toward a solid, ACC like form follows a downhill energetic sequence, similar to the dehydra tion and subsequent crystallization of ACC.[41]

Our group has primarily focused on the polymer induced liquid precursor (PILP) process and its relevance to biomineralization. In this case, the liquid precursor phase exists long enough to be manipulated into non equilibrium morphologies, the hallmark of biominerals. Thus, it is highly desirable to understand what the mechanistic role of the polymer is in this process in light of these other new findings of various precursor phases. For example, rather than the polymer interacting with ions, as we had originally assumed, one must now consider if the polymer might actually be interacting with any of these other species that have been detected in $CaCO_3$ solutions.[23 25] Thus, the focus of this paper can be expressed in two parts: 1) without polymer additives, can the $CaCO_3$ liquid precursor be detected at a more neutral and biologically friendly pH of 8.5? 2) Does PILP form through poly mer interaction with a pre existing liquid precursor, with PNCs (as previously proposed),[42] or by some other interaction?

Given this focus, we carried out studies of the early stages of precipitation in a fashion similar to Gebauer *et al.*, except that we conducted our studies at pH 8.5 and allowed the ever increasing supersaturation to evolve by using punctuated injec tions of aqueous $CaCl_2$ into bicarbonate buffer, allowing for time between injections to allow for system equilibration. At various points in the evolution, we analyzed the state of the solution using a Ca^{2+} ion selective electrode, isothermal titration calorim etry (ITC), nanoparticle tracking analysis (NTA) light scattering, analytical ultra centrifugation (AUC) and carbon specific nuclear magnetic resonance (^{13}C NMR) spectroscopic techniques such as Carr Purcell Meibloom Gill (CPMG) T_2 measurement and pulsed field gradient stimulated echo (PFG STE) diffusion NMR. It should be noted that we did not modulate the pH during the supersatura tion evolution as did Gebauer *et al.* The PILP generating technique used in our lab that we wished to model does not maintain a constant pH. Rather, we allowed the

pH to evolve with the titration and monitored it throughout the titration. Using these methods at a moderate pH of ~8.5, we discovered a new phase transition of a liquid condensed phase (LCP) that occurs at a critical concentration of bound calcium. We then used the same techniques with a polymer (polyaspartic acid sodium salt) present to determine if the formation of the polymer induced liquid precursor (PILP) phase is indeed a polymer stabilized LCP phenomenon.

Materials and methods

Generation of super-saturated solution in the absence of polymer additive

Using a micropipette, 20 mM sodium carbonate (Fisher) was titrated into a 20 mM sodium bicarbonate (Fisher) solution to generate a 20 mM, pH 8.5 carbonate buffer solution. Calcium chloride (Fisher) solution with a concentration of 4.5, 6, or 10 mM was titrated into 29 ml of carbonate buffer, which was stirred at 100 rpm using a magnetic stir bar. The volumes of titration were 200 μl each except for the first injec tion which was only 40 μl to account for infinite dilution phenomenon. Titrations were injected at an approximate rate of 20 μl s ^{1} immediately over the rotating stir bar to ensure adequate mixing. The titrations were made in a punctuated fashion, 2 min of constant pH, and $[Ca^{2+}]_{Free}$ measurements were acquired before injecting more $CaCl_2$(aq). The solutions were prepared with nanopure water and all were filtered using a 0.22 μm Millipore syringe filter prior to any titrations. Each of these titrations was conducted in triplicate and the error expressed in the results is plus or minus two standard deviations.

Generation of super-saturated solution in the presence of polymer additive

Using a micropipette, 300 mM sodium carbonate was titrated into a 300 mM sodium bicarbonate solution to generate a 300 mM, pH 8.5 carbonate buffer solution. This solution was then titrated into 29 ml of a stirred 10 mM $CaCl_2$ solution which may or may not contain 20 μg ml ^{1} polyaspartic acid sodium salt (monodisperse, Alamanda Polymers), depending on the experiment. The volumes of titration were 200 μl each except for the first injection which was only 40 μl, matching the titration conditions for the non additive experiments. Titrations were injected at an approximate rate of 10 20 μl s ^{1}, always over the rotating stir bar to ensure adequate mixing and to mini mize the formation of strong concentration gradients that might affect the experi ments. The titrations were made in a punctuated fashion; 2 min of constant pH, and $[Ca^{2+}]_{Free}$ measurements were acquired before injecting more titrant. The injec tions were made using disposable micropipette tips that were disposed of after each injection and replaced prior to a new injection. Each experiment was conducted in triplicate, including the control, and the error shown is plus or minus two standard deviations.

Ca^{2+} electrode and pH electrode measurements

The free Ca^{2+} concentration, $[Ca^{2+}]_{Free}$, in the titrated solution was obtained using a Ca^{2+} ion selective electrode (Radiometer Analytical, ISE K Ca, E11M006) in conjunction with a reference electrode (Radiometer Analytical E21M009). A cali bration standard curve for calculating free Ca^{2+} concentration was generated by titrating the experiment appropriate concentration of $CaCl_2$(aq) into nanopure water which had been brought to pH 8.5 by the addition of trace amounts of NaOH (Fisher) (aq). The pH evolution of the titration was obtained using a stan dard pH electrode. Both pH and $[Ca^{2+}]_{Free}$ values had to remain constant for at least 2 min of mixing before adding another titration injection to verify that the solution equilibrated and that solid nucleation had not yet occurred. It is important to note that we are not quantitatively accounting for CO_2 net diffusion out of the solutions during our experiments.

Isothermal titration calorimetry (ITC) of phase transition

All measurements were made using a VP ITC (MicroCal™). Carbonate bicarbonate buffer and $CaCl_2$(aq) was generated as described above. The injection of $CaCl_2$(aq) into the reservoir carbonate bicarbonate buffer was maintained at exactly the same ratio as the titration experiments to give exact punctuated enthalpies that corre spond to the titration experiment. The experiments were conducted at a controlled temperature of 298 Kelvin. The rest time between injections was adjusted to allow for complete thermodynamic equilibration between the reaction vessel and the refer ence vessel. A stir speed of 180 rpm was used for all the experiments. A reference power of 2 μcal s^{-1} was used due to the very subtle, endothermic nature of the reac tion. The solutions were not degassed due to the fraction of CO_2 that is in equilib rium within the carbonate bicarbonate buffer at pH 8.5. No bubbling phenomena were observed during the course of the ITC experimentation. Control enthalpy profiles of $CaCl_2$(aq) injections into water, water injections into bicarbonate buffer, and water injections into water were subtracted from the raw data to normalize the data.

Nanoparticle tracking analysis (NTA) of emergent phase

The number count and the hydrodynamic radius of the emergent phase droplets were analyzed using the NTA light scattering technique. Samples were analyzed using an LM20 analyzer (Nanosight™) and the data was processed using an NTA analytical software suite (Nanosight™). Samples for analysis were prepared as described in the "Generation of super saturated solution" section. 0.3 ml of sample was used in each analysis.

Analytical ultracentrifugation (AUC)

AUC was performed on an Optima XL I (Beckman Coulter, Palo Alto, CA) using the Rayleigh interference optics at 60 000 rpm and 25 °C. The experiments were per formed in 12 mm titanium double sector cells (Nanolytics, Potsdam, Germany). All experiments were evaluated using the software SEDFIT applying Lamm equation modelling for 1 4 noninteracting species to determine sedimentation and diffusion coefficients as well as concentration of up to 4 species in a solution.[43,44]

NMR, PFG-STE, spin spin (T_2) relaxation time measurement

All NMR experiments were conducted on a Bruker Avance DRX 500 MHz vertical bore system using a *xyz* gradient TXI probe with a 1H and 2H interior coil, ^{13}C and ^{15}N exterior coil, and *xyz* gradients. All carbonate bicarbonate buffer solutions were generated as described above except using 100% ^{13}C enriched sodium carbonate and sodium bicarbonate ingredients (Cambridge Isotopes) to enhance signal/noise. All experiments were conducted at 298 Kelvin. Deuterium oxide was used to obtain a lock at a volume fraction of 2.5% of the total sample. Data was processed using TOPSPIN™ software and MATLAB™ derived software when deconvolution of overlapping spectral peaks was required. The T_2 relaxation times of the various species in solution were obtained using a Carr Purcell Meibloom Gill (CPMG) sequence with increasing tau (τ) times of 40, 120, 200, 400, 600, 800, 1000, 2000, 3000, and 4000 msec. PFG STE ^{13}C diffusion experiments were conducted using the variation of the Bruker stegs1s pulse sequence based upon the pulsed field gradient spin echo (PFG SE) technique for measuring diffusion. ^{1}H was decoupled from ^{13}C for the entirety of the pulse sequence. We used 1.8 s diffusion times and 1 msec gradient pulse times. All processing was zero filled twice and was done with 0.3 Hz line broadening to allow for characterization of NMR spectral features. We used a gradient with strength of 50 g cm^{-1} for the gradient pulses which were varied equi distantly between 2% and 95% to generate 16 1 D slices for analysis. The PFG STE

pulse sequence used, as well as many of the relevant variables chosen, is shown in Fig. S.1† of the supplementary information.

Results

Metastable liquid condensed phase (LCP)

The binding behavior of Ca^{2+} ion as aqueous $CaCl_2$ was titrated at various concen trations into 20 mM carbonate buffer (pH 8.5) is shown in Fig. 1a. Even though care was taken to minimize temporary concentration gradients when introducing Ca Cl_2(aq) to the bicarbonate buffer, there still appear to be some kinetic effects due to the injection. This is evident by the slight difference in binding fraction between the various concentrations of $CaCl_2$(aq) injectant. The bound fraction (slope of the displayed line) would be expected to be very similar if the system were at true ther modynamic equilibrium. Therefore, interpretation of the data should be approached from a qualitative standpoint. To additionally demonstrate the kinetic binding effects that can occur due to imperfect addition of ion to counterion, and to elimi nate the possibility that the character of the Ca^{2+} binding profiles are due to nucle ation of mineral at the nozzle (micropipette tip), an additional titration was performed with the nozzle just above the solution. The results, shown in Fig. S.2† of the supplementary information, demonstrate that the qualitative character of the Ca^{2+} binding profile is conserved and not due to nucleation at the nozzle even if kinetic binding effects are enhanced. Additionally, we did not quantitatively

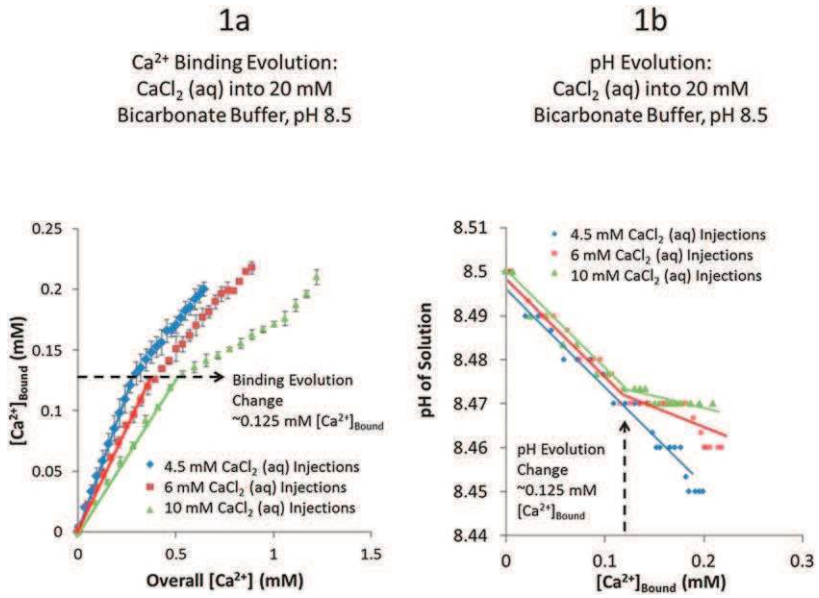

Fig. 1 Left (1a) the evolution of bound Ca^{2+} *vs.* overall titrated [Ca^{2+}] as $CaCl_2$(aq) is titrated into 20 mM carbonate buffer, pH 8.5. Initially, the binding profile is linear which is expected for prenucleation cluster formation. However, a discontinuity in Ca^{2+} binding is observed at a value of ~0.125 mM $[Ca^{2+}]_{Bound}$, which is evidence of a phase transition. The evolution was done in triplicate and results were averaged. Right (1b) the pH evolution of the pH 8.5 20 mM bicarbonate buffer system due to the injection of $CaCl_2$(aq). The pH decreased due to the consumption of CO_3^{2} to form ion pair PNCs until a discontinuity occurs at a consistently measured $[Ca^{2+}]_{Bound}$ of ~0.125 mM, further suggesting a phase transition at the same bound calcium concentration. The change in pH evolution in the upward (basic) direction suggests that a larger fraction of bicarbonates and/or a reduction of carbonates are participating in Ca^{2+} binding. Lines were included as an aid.

account for carbon dioxide gassing out that would occur with this solution over time. This can lead to changes in binding affinity and pH over time. For these reasons, we interpreted the data qualitatively.

Initially, during the titration, the fraction of calcium that binds is constant with each additional injection, which is expected for the formation of calcium carbonate prenucleation clusters.[20] However, at a critical bound calcium concentration (~0.125 mM in this case), the constant Ca^{2+} binding affinity decreases yielding a new linear binding affinity slope, suggesting a change in the types of products forming. Note this change in binding behaviour occurs prior to solid nucleus formation, which would be evidenced by the inability to achieve apparent equilibrium due to decreasing pH (massive carbonate binding) and decreasing free calcium concentra tion (massive binding of Ca^{2+} to form solid mineral). Interestingly, at the point of the transition, the $[Ca^{2+}]_{Free}[CO_3^{2}]_{Free}$ ion product is different for all three Ca Cl_2(aq) titration concentrations (0.4, 0.7, 0.1 mm^2 for 4.5, 6, and 10 mM injections, respectively). Solid nucleation and growth leading to precipitation eventually occurred at concentrations of bound Ca^{2+} between 0.2 and 0.22 mM.

The pH evolution of the solution was monitored during the titration and the results are shown in Fig. 1b. The pH of the solution was decreasing initially, as would be expected, prior to the phase transition due to the sequestering of CO_3^{2} carbonate ions as predicted to occur during PNC formation. The pH evolution flat tened considerably at the same bound Ca^{2+} concentration (~0.125 mM) as the change in binding affinity was observed, indicating that the Ca^{2+} binding affinity to bicarbonate has increased relative to carbonate. As nucleation is a singular event, the discontinuity in the pH development and/or the change in Ca^{2+} binding develop ment strongly points toward the nucleation of a second phase. Because the pH devel opment becomes flatter, less carbonate, or more bicarbonate ions are binding after nucleation of this phase, suggesting that the bicarbonate ion is participating in the emergent phase. The data displayed in Fig. 1 suggest that there is a critical bound calcium concentration that leads to a phase transition which involves the bicar bonate ion.

In order to gain further insight into the thermodynamics of this phase transition, isothermal titration calorimetry (ITC) was conducted using the same punctuated titration method as was used for the Ca^{2+} binding and pH development experiments to measure the enthalpy change upon nucleation of the emergent phase. All three titration concentrations were tested, and as can be seen in Fig. 2, a first order phase transition, identified by the apparent enthalpic discontinuities, is occurring at similar conditions as identified in the titration experiments, further corroborating the notion that a phase transition has occurred. The phase transition occurred 3 injections earlier for the 4.5 mM injection and 2 injections early for the 6 mM injection in the ITC experiment as compared to the desktop titrations, possibly due to the more controlled environment of the ITC reaction chamber. The enthalpic disconti nuity is positive, demonstrating that the driving force of the phase transition is entropic, which is often a sign of liberation of hydration waters.

Nanoparticle tracking analysis (NTA) was used to examine the size of the emer gent phase species and to estimate the amount of species in solution after the phase transformation. Samples were analyzed prior to, at, and after the observed phase transition (the 7th, 10th, and 13th injection, respectively) for the case of the 6 mM $CaCl_2$ titrant. The results of the analysis are shown in Fig. 3. Prior to the detected phase transition (7th injection), no phase was detectable since pre nucleation clusters of *ca.* 2 3 nm in diameter are well below the 20 nm diameter threshold for the NTA method and therefore there isn't any data for this condition to present. At the de tected phase transition (the 10th injection), large species emerged with a diameter size distribution of ~60 nm. Additional $CaCl_2$ injections (13th injection) resulted in an increase in size of up to 100 nm diameter, suggesting that increasing Ca^{2+} concentration leads to growth and/or coalescence of the emergent phase. This strongly suggests that the emergent phase is stable with respect to the solution

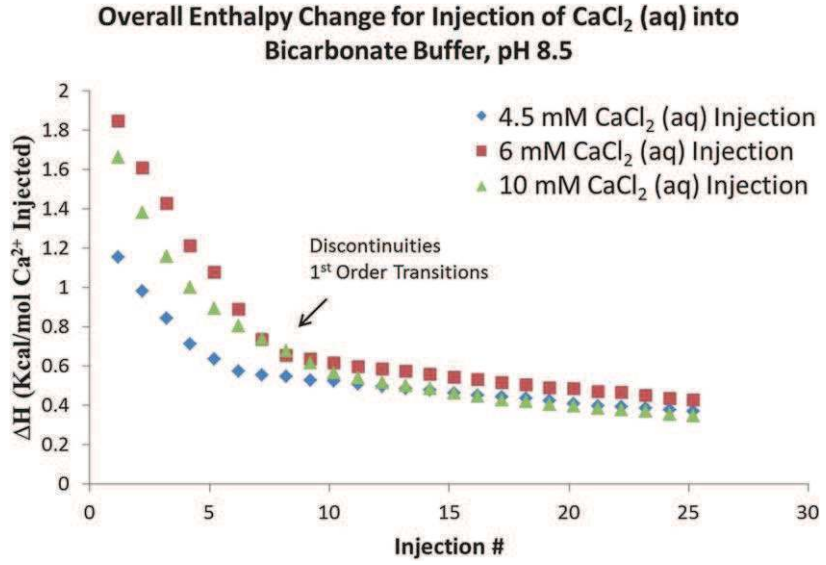

Fig. 2 The enthalpy of reaction during the titration of $CaCl_2$(aq) into 20 mM carbonate buffer, pH 8.5. The data shows that there is an endothermic phase transition occurring, indi cating that the phase transition is entropically driven and probably due to liberation of hydra tion waters.

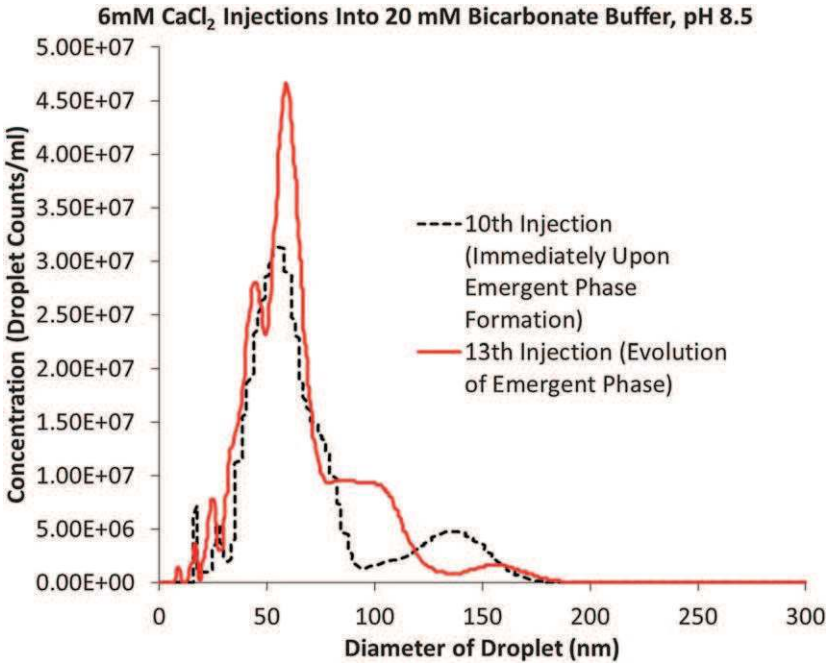

Fig. 3 The emergent phase size distribution, according to nanoparticle tracking analysis (NTA), of the solution at and after the phase transition (injection 10 and 13, respectively for a 6 mM $CaCl_2$(aq) injection). Prior to the phase transition no species were detected. At the phase transition (10th injection), droplets with a distributed diameter averaging ~60 nm emerge. The addition of more Ca^{2+} to the solution yields more detectable phase emerging at 60 70 nm diameter and they seem to grow larger as well.

species, because if it were metastable, it could only occur in the form of microscopic fluctuations in the solution and would not grow with further Ca^{2+} injections.

A video of the raw data used to track the scattering phase is shown in the supple mentary information Fig. S.3.† In the video one can see that the droplets showed somewhat unusual behaviour, almost as if the species were warping and adopting a temporary aspect ratio. The species were not observed to coalesce or split perma nently; they came close to doing so and then re established the former interfaces prior to the interaction. This behavior seems consistent with the Wolf *et al.* observa tion of $CaCO_3$ precursor droplets having emulsion like behavior with a resistance to coalescence due to weak electrostatic stabilization.[45] According to the NTA results, the emergent species is very dilute (on the order of 10^{12} species liter ^{1}), which suggests that the aggregation/coalescence of particles/droplets that yield the emer gent phase arises due to weak interactions. Note this phase would be difficult to detect using standard dynamic light scattering techniques, which require a much higher particle/droplet count and a known refractive index.

Analytical ultracentrifugation (AUC) was used to detect the species present in solution for the various points of $[Ca^{2+}]$ evolution for the case of the 6 mM Ca Cl_2(aq) injection. The results are presented in Fig. 4. Prior to the emergent phase formation, ions/ion pairs and PNCs are present as indicated by the squares and circles, respectively. At the expected point of phase emergence, larger species suddenly emerge (D & E in Fig. 4). After a few more injections, only ions/ion pairs are detected. This result seems counterintuitive after a phase transformation, but if the volumes of the phases are considered, it becomes understandable. As determined by NTA analysis, the LCP droplets are very dilute and represent a very small frac tion of the overall volume. Literature reports on emulsion systems demonstrate coa lescence with subsequent demixing allowing for a determination of the respective phase volumina.[46] However, the small volume fraction of this newly formed liquid phase with respect to the mother solution, would lead to an undetectable phase boundary and therefore, only the ions and prenucleation clusters in the major liquid phase can be seen. Due to the apparent liquid nature of this emergent phase as in ferred from the NTA and AUC analyses, we refer to these as liquid condensed phase (LCP) droplets.

Nuclear magnetic resonance was used to further analyse the constituents involved in the LCP in comparison to the solvated carbonate bicarbonate species in the bulk

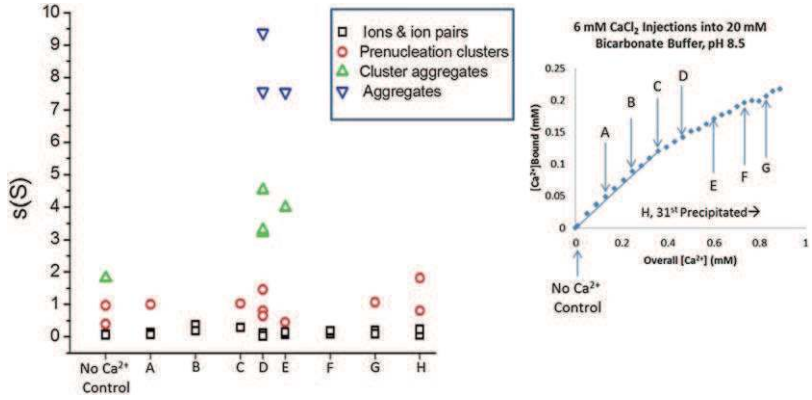

Fig. 4 Sedimentation coefficients (25 °C) for the detected species in solution by AUC for the injections indicated in the inset. The emergence of LCP occurs at point C. It is evident that larger species are present for D & E, just after the phase transition. The control consists of just carbonate buffer. PNCs are also seen in the control because they can form with sodium carbonate species as well.

solution. Specifically, Carr Purcell Meiboom Gill (CPMG) spin echo and pulse field gradient stimulated echo (PFG STE) diffusion NMR techniques were em ployed. CPMG measures the T_2 relaxations, which investigates the immediate surrounding chemical environment of the species. PFG STE measures the self diffu sion of the carbonate bicarbonate species. Self diffusion is the diffusion coefficient of a species in the absence of any chemical potential gradient but for our situation it is synonymous to the translational diffusion coefficient. Firstly, it should be noted that a 1D spectrum of the system after the phase transition (17 injections of 6 mM $CaCl_2$(aq) titrant shown in Fig. 5) does not indicate the presence of solid precipitation products at the $CaCO_3$ or $Ca(HCO_3)_2$ predicted chemical shifts. Solids would result as a broad NMR spectrum with a carbonate peak at ~170 ppm or a bicarbonate peak at ~160 ppm, which are not observed. However, if the carbonate bicarbonate is behaving as a solvated solute or a dynamic liquid, then they can interconvert through proton exchange and the result is an intermediate NMR spectrum, with one peak in between the two chemical shifts due to rapid (de)protonation interconversion between the two states.[47,48] Thus, NMR provides additional independent evidence of the liquid character of the nucleated LCP phase. The emergent LCP phase is further evident by the distortion of the resultant peak resulting in an asymmetric broadening and "bulging" of the peak in the up field direction (bicarbonate direction) (Fig. 6). There is a slight widening seen in the 7th injection prior to the phase transition as compared to the buffer control but it is minor and very symmetric, suggesting the presence of only one phase. The asym metric upfield direction bulging of the solution with 17 injections of $CaCl_2$(aq) suggests that this portion of ions is favouring bicarbonate in the bicarbonate carbonate interconversion to a greater extent than the bulk solution and that there may be an additional phase in the system. This is consistent with the pH measure ment shown in Fig. 1b, which also suggests a favoring of bicarbonate binding (or a less pronounced carbonate binding) after the phase transition. We do not consider this emergent asymmetric bulging to be due to the aggregation of PNCs alone, because of its bicarbonate favored directionality. Also, the dynamics of PNCs is re ported as being on the order of pico and nano seconds, which would be far too short to resolve from the bulk solution over time averaged data of 5.5 s for these NMR experiments.

The broadened peak was deconvoluted for analysis using Gaussian distributions to model overlapping peaks, resulting in a bulk solution peak (main peak) which resembles in width and chemical shift the carbonate buffer control, and an emergent

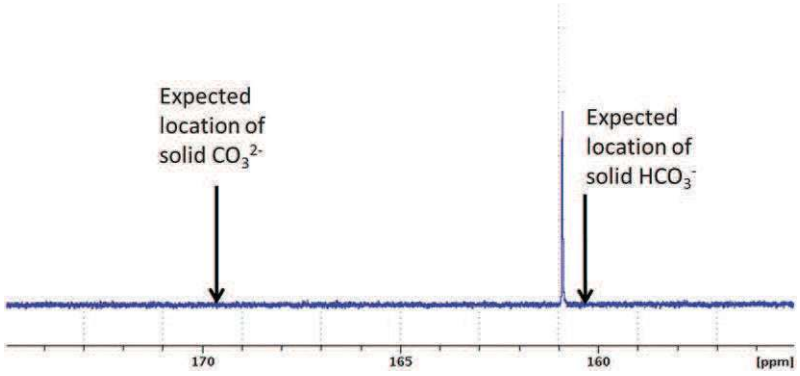

Fig. 5 A 1 D ^{13}C spectrum of the solution after the phase transition (17th injection of 6 mM $CaCl_2$(aq) into 20 mM carbonate buffer, pH 8.5). There are no detectable peaks at the solid carbonate or bicarbonate chemical shifts (marked with arrows). The effect of the nucleated liquid precursor phase is seen as a widening of the peak because it is still behaving as a (non solid) phase.

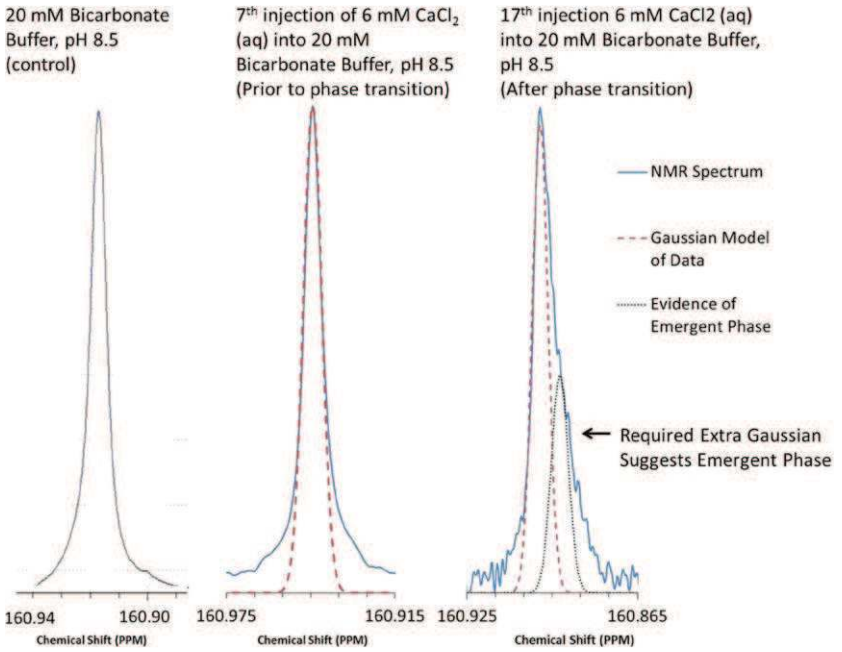

Fig. 6 (Left) 1 D NMR ^{13}C spectrum of 20 mM bicarbonate buffer, pH 8.5 (control). (Center) First slice of the ^{13}C NMR T_2 measurement of the 20 mM bicarbonate buffer with 7 injections of 6 mM $CaCl_2$(aq). (Right) First Slice of the ^{13}C NMR T_2 measurement of the 20 mM bicarbonate buffer with 17 injections of 6 mM $CaCl_2$(aq) (after phase emergence). Both the control (left) and the solution prior to phase transition (center) symmetrical Gaussian distributions of signal. After the phase transition (right), the evidence of an emergent phase manifests as an asymmetric bulge shifted upfield from the bulk solution peak which requires an additional Gaussian peak to model. The data was deconvoluted in order to attribute T_2 relaxation measurements and ^{13}C NMR diffusion measurements to each modeled portion of the peak.

peak (small peak) which is suspected to be the emergent liquid condensed precursor phase (see Fig. 6). To see an example of our Gaussian modelling of overlapping peaks, see Fig. S.4† of the supplementary information. Measuring the T_2 relaxation and diffusion properties of the carbonates and bicarbonates in the buffer solution by means of NMR is an excellent way to establish that there are distinctly different species present after the phase transition. The T_2 relaxations of both deconvoluted peaks were determined by using the CPMG technique, which measures the reduction in peak intensity (M/M_0) *vs.* the change in the tau delay according to the following equation:

$$ln\left(\frac{M}{M_0}\right) = \frac{\tau}{T_2} \quad (1)$$

The result is a linear relationship between the natural log of the signal attenuation and the tau delay with a slope of $1/T_2$ which can be found by fitting the data. The results, shown in Fig. 7(top), show that the average T_2 relaxation of 0.9 s for the ions associated with the LCP is much faster than the average bulk solution ions T_2 relaxation of 1.5 s, suggesting that the emergent ions expressing bicarbonate bias are tumbling at a different rate and/or are in a different chemical environment than the ions making up the bulk solution over several second time averages. The bulk solution T_2 relaxation of 1.5 s is identical to the T_2 relaxation that was obtained for pure carbonate buffer suggesting that the carbonate bicarbonate ions making

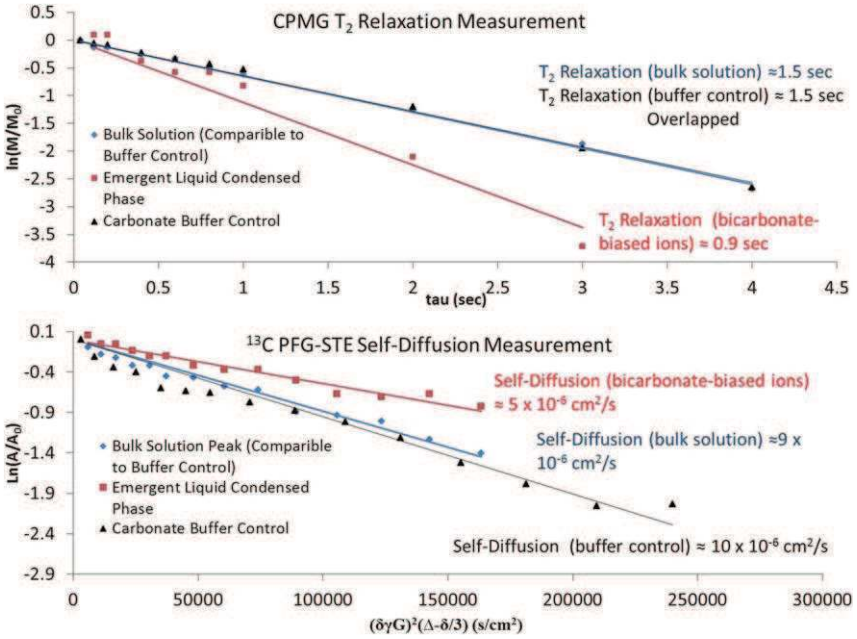

Fig. 7 The results of the CPMG T_2 relaxation measurement (top) and the ^{13}C PFG STE self diffusion measurement (bottom) of the deconvoluted NMR peaks. The CPMG plot (top) is plotting the reduction in peak intensity (left side of eqn (1)) *vs.* the tau delay (right side of eqn (1)). The result is a linear relationship with a slope of $1/T_2$. The diffusion measurement plot (bottom) plots the degree of attenuation (left side of eqn (2)) *vs.* the right side of the equation, where the slope of the resulting line is D (negative diffusion constant). The bicarbonate biased ions (bulge) have a shorter T_2 relaxation time and a slower diffusion, suggesting that a fraction of the carbonate bicarbonate ions are slowed in rotation and in diffusion, presumably due to interactions with Ca^{2+} and the emergent LCP. The self diffusion of the bulk solution carbonates bicarbonates is roughly the same as the self diffusion of carbonate buffer alone ($\sim 10 \times 10^{-6}$ cm^2 s^{-1}).

up the bulk solution are tumbling and/or are in a chemical environment similar to bicarbonate buffer control (control) (shown in Fig. S.5† of the supplementary information). T_2 relaxations of solvated, ^{13}C enriched, carbonate bicarbonate solutions like the ones discussed in this paper are primarily due to chemical shift anisotopy (CSA). Chemical shift anisotropy occurs if the electron shielding around the dipole is anisotropic, as is the case of asymmetric carbonate and bicarbonate ions. When CSA is present, the extent to which the dipole interacts with an applied magnetic field depends on the rate of molecular tumbling of a dipole. In dilute, non viscous solution states, the effect of CSA is often averaged out due to rapid tumbling of molecules. When carbonates/bicarbonates rotations are inhibited by interactions/binding with Ca^{2+}, the reduced tumble rate of molecules enhances the CSA effect and leads to a reduction of T_2 relaxation times. The relaxation rates of the Ca^{2+} bound/interacting carbonates and bicarbonates are on the order of solution state relaxations. Solids have much shorter T_2 relaxations, on the order of less than a millisecond, and therefore, the detected bicarbonate biased ions exhibit solute character, which may rely on the internal rapid dynamics of the liquid calcium carbonate precursor phase.

As mentioned above, ^{13}C PFG STE diffusion NMR is an excellent non invasive technique for establishing the co presence of two distinct diffusions within a solution, indicating the presence of an emergent liquid phase. In the case of this study, we assumed isotropic, unbiased diffusion and therefore were concerned only with

diffusion rates in the z direction (measured by the magnetic field gradient created in the z direction). The nucleus of interest, in this case the ^{13}C nucleus of carbonate bicarbonate, is subjected to a 90° pulse for an encoding step, followed by another 90° pulse to store the magnetization. After an evolution time (diffusion time), a final 90° pulse is applied after the evolution time to refocus the transverse magnetization for acquisition. A field gradient of amplitude, G and duration, δ, is applied during the first and third 90° pulses to apply and remove, respectively, the spatial encoding to the ^{13}C nuclei. This ensures that the extent of refocusing of the applied 90° encod ing pulse is dependent on the degree of deviation from the initial position that was spatially encoded by the gradient. Translational movement of the dipole during the diffusion time results in an attenuation of the intensity of signal (A/A_0) which is related to D (the self diffusion constant) through the following expression:

$$ln\left(\frac{A}{A_0}\right) = D(\delta\gamma G)^2\left(\Delta \quad \frac{\Delta}{3}\right) \tag{2}$$

where G is the gradient strength, γ is the gyromagnetic ratio of ^{13}C, δ is the duration of the gradient application, and Δ is the diffusion time. By plotting the left side of the equation *vs.* the right side with stepwise increases in the gradient strength, G, we generated a line with slope D (negative self diffusion constant), as seen in Fig. 7(bottom). This figure compares the diffusions of the emergent LCP (obtained by 17 injections of 6 mM $CaCl_2$(aq) into 20 mM bicarbonate buffer, pH 8.5) with the mother bulk solution and a bicarbonate buffer control. This required the deconvo lution of NMR spectra in a similar fashion as described for the T2 determination above. A description of the method and the attenuation of signal are shown in Fig. S.6† of the supplementary information. The results indicate two distinct diffu sions exist in the LCP containing solution, a slower one of 5×10^{-6} cm^2 s^{-1}, which is attributed to bicarbonate biased ions contributing to the emergent phase, and a faster one of 9×10^{-6} cm^2 s^{-1}, which is that of the bicarbonates carbonates in the bulk solution. The self diffusion of the bulk solution peak is very similar to the diffu sion we obtained from our control of carbonate buffer alone (10×10^{-6} cm^2 s^{-1}), and is in close accordance with literature values for the self diffusion of carbonate buffer obtained by simulation[49] and by experiment[50] under similar conditions. It should be noted that the slower diffusion attributed to the emergence of a LCP is not that of the large LCP droplets seen using the NTA technique which, given their size of >60 nm, would be orders of magnitudes slower based on Einstein Stokes diffusion (and not detectable with the gradient used in this experiment), but rather are believed to be that of small Ca^{2+} bound carbonate bicarbonate ion pair species that might be constituents of the large metastable droplets. According to the Einstein Stokes equation (using the kinematic viscosity of water at 25 °C), the bulk solution and buffer control carbonates bicarbonates have an effective diameter of 0.5 nm. The slower diffusing carbonates bicarbonates have an effective diameter of 1 nm. The favouring of bicarbonate, the apparent slowing of ^{13}C based ion rotations, and the roughly doubling of effective diameters suggests that there is a significant amount of calcium bicarbonate monodentate and calcium bicarbonate bidentate ion pairing phenomenon present, which are being detected over relatively long time averages as compared to the bulk mother solution.

Another interpretation is that the emergent LCP is more viscous than the mother solution. The average effective size of the detected carbonate bicarbonate may be a singular ion still if the viscosity of the emergent phase were twice that of water, or about 0.018 dyne sec cm^2. Both interpretations suggest that there is a liquid liquid separation occurring that is forming a LCP. It is important to stress that the effective diameters calculated are based on diffusion of the ions, which are expected to be an ensemble average due to the dynamic nature of ion pairs and PNCs and free ions along with their associated waters of hydration. This needs to be considered when comparing these values to the size of PNCs determined by means of cryo TEM[21]

and AUC.[20] However, the average diameter of the Ca bicarbonate biased ion pairing species in our 2 phase system of 1 nm is relatively consistent with the diameters of 0.75 nm and 2.0 nm obtained by cryo TEM and AUC, respectively.

The data as a whole suggests that, at a critical bound Ca^{2+} concentration, Ca bicarbonate ion pairs begin to associate due to entropic driving forces (often the liberation of hydration waters) into a sparse, but visible, metastable liquid condensed phase. Due to evidence of LCP droplet growth during experiment evolu tion, the phase is believed to be stable with respect to the solution state. The bound Ca bicarbonate species believed to comprise the LCP appear to have a long enough dynamic lifetime to be detectable using solution state NMR, (unlike PNCs), and they appear to be slowly translating in space and slowly tumbling as compared to the free carbonate bicarbonate in the bulk solution. It is reasonable to assume that the emergent droplets are comprised of bicarbonates given the data, but, consid ering how dispersed the droplets are, the bulk of the detected bicarbonate bias species being detected by the NMR must be in solution, possibly exchanging onto and off of the droplets. It is important to point out that the values of T_2 and self diffusion obtained by NMR are on the scale of solutes in solution, supporting the notion that the LCP is a liquid phase distinct from the mother solution. The values of T_2 and self diffusion for solids would be many orders of magnitude smaller.

Experiments in the presence of polyaspartate

In the titration and NMR experiments, the method of generating a super saturated solution with polymer additive differed from that without additives. The reason for this was to mimic our lab's convention of adding carbonate bicarbonate ion to a solution containing $CaCl_2$ and polymer additive to initiate the PILP process. Also, the polymer additive has such a strong stabilizing effect on the solution that the concentration of bicarbonate buffer needed to be increased to generate a suffi cient super saturation to observe eventual solid nucleation and precipitation.

A Ca^{2+} binding profile, in the presence of PAsp (14 000 g mol $^{-1}$ and 27 000 g mol $^{-1}$ MW), as 300 mM bicarbonate buffer, pH 8.5 was titrated into a 10 mM $CaCl_2$, 20 μg ml $^{-1}$ PAsp solution is shown in Fig. 8. As is the case with Fig. 1, there is presumably some kinetic binding effects occurring in this titration and therefore the Ca^{2+} binding profile should be treated as qualitative. As a control, a Ca^{2+} profile was conducted for a titration in the absence of PAsp for comparison. In this case, one can see an apparent discontinuity in Ca^{2+} concentration at an early stage that is analogous to the one seen in Fig. 1a. As with the discontinuity shown in Fig. 1a, this potential discontinuity suggests that a phase transition has occurred. In order to aid in visu alization, lines have been added to the inset of the figure to demonstrate disconti nuity.

In the presence of polymer, the first thing that one notices is how much farther the Ca^{2+} profiles extend prior to precipitation relative to the control (bottom curve, with no polymer). In addition to this stabilizing influence, the shapes of the titration curves show an interesting trend. The binding of Ca^{2+} with respect to injections of $CaCl_2$ (aq) appears to display a discontinuity (Fig. 8, inset), suggesting that LCP is forming in the presence of polymer as well, as evidenced by the same type of discontinuity as seen in the non additive case (Fig. 1a). The LCP like Ca^{2+} binding behaviour continues for many more injections beyond where the additive free control would have precipitated (see precipitation indicators in Fig. 8). The contin uation of the same type of binding that forms the LCP phase is a strong indication that LCP is being stabilized by the presence of the PAsp polymer additive. Thus the polymer's role in the PILP process may be to stabilize the LCP.

It is relevant to note that Verch *et al.*, in a "fingerprinting" study on the effect of polymer additives, also detected a significant nucleation inhibition and a species after nucleation of $CaCO_3$ in presence of PAsp (MW 6800 g mol $^{-1}$ and MW

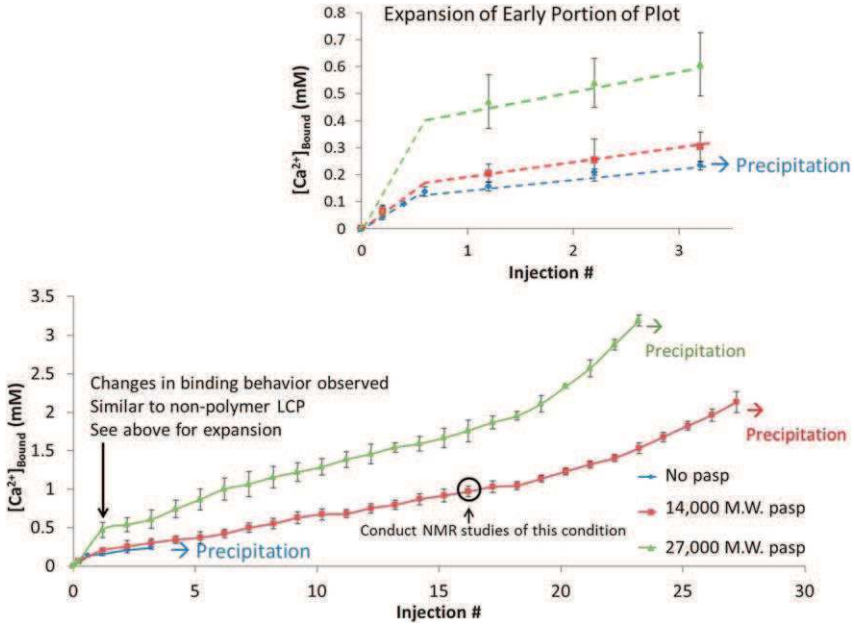

Fig. 8 The $[Ca^{2+}]$ profile of a system where 300 mM bicarbonate buffer, pH 8.5 was injected (40 μl initial, 200 μl for the rest) into 10 mM $CaCl_2$ with 20 μg ml ^{1} PAsp (no PAsp for control). The results qualitatively show evidence of a phase transition and are analogous to the LCP formation in the absence of polymer shown in Fig. 1a. After the presumed LCP formation, the solution is stabilized against solid nucleation and precipitation for many more injections, suggesting that LCP is stabilized due to the interaction of polymer with the LCP phase. This may be the basis for the PILP process. NMR studies to analyze the two phases in solution (bulk solution and phase separated PILP) were conducted at the location indicated by the circle.

27 000 g mol ^{1}) that is much more soluble than ACC, which they related to a PILP phase (although they worked at a higher pH of 9.75).[51]

A profile of the pH evolution with the addition of 200 μl injections of 300 mM, pH 8.5 bicarbonate buffer into 10 mM $CaCl_2$(aq) containing 20 μg ml ^{1} of PAsp is shown in Fig. 9. It is apparent when comparing the pH evolution of bicarbonate buffer into aqueous PAsp solution (diamonds and squares) to the pH evolution of bicarbonate buffer into pure water (dotted orange line) that PAsp has a damp ening effect on the evolution by maintaining a lower pH. This leads to a higher bicarbonate : carbonate ratio at the early points in the titration. This would be a very effective means for directing more bicarbonate to bind with Ca^{2+} if it were present. When Ca^{2+} is present with the PAsp (triangles and crosses) the pH development suggests this is the case. In comparison to the controls in the absence of Ca^{2+}, the Ca^{2+} containing solutions actually do demonstrate additional bicarbonate binding in terms of a bicarbonate : carbonate ratio, until a certain threshold is met. At this point the pH evolution flattens considerably at a much lower pH than the various controls. This supports the assertion that a critical amount of Ca bicarbonate ion pairs accumulates leading to a phase transition (LCP) and a change in Ca^{2+} affinities for bicarbonate and carbonate. The prefer ence to maintain a pH in the range of a lower 8s supports the view that an emer gent bicarbonate rich phase is participating in directing the binding preference for Ca^{2+}. Fig. 9 supports the view that PAsp (and potentially other additives) promote and stabilize the LCP phase and perhaps is the description for the so called PILP process.

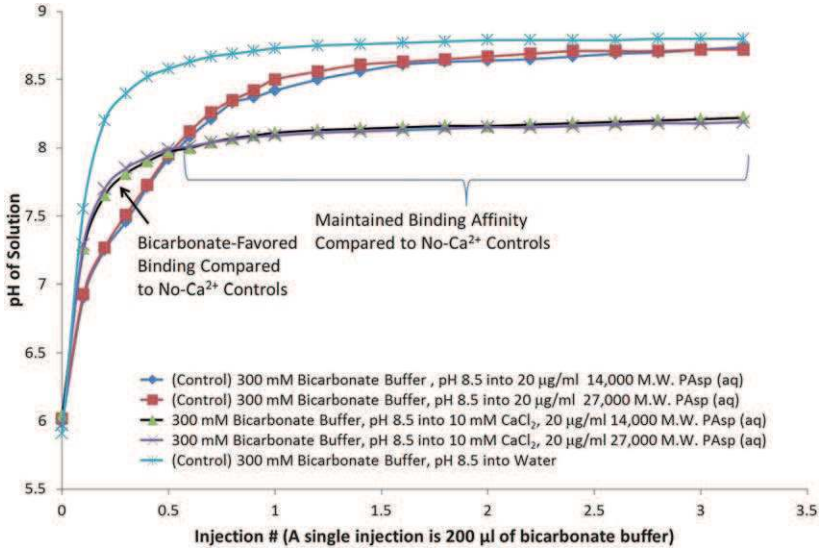

Fig. 9 The pH evolution of a 10 mM $CaCl_2$ solution containing 20 µg ml ^{1} PAsp due to the punctuated titration of 300 mM bicarbonate buffer, pH 8.5. The presence of PAsp has a miti gating effect on the upward evolution of the solution, allowing for more bicarbonates to be present (diamond and squares). When Ca^{2+} is present with the PAsp, the pH evolution increases in the basic direction faster than the evolution with PAsp alone, before leveling off at a preferred pH. This suggests that when enough bicarbonate has bound, an equilibrium is estab lished, presumably due to an emergent phase, resulting in a consistent, flattened pH evolution. The typical injection is 200 µl, but to characterize the early titration, fractions of 200 µl injec tion were used.

To analyse the PILP phase which is suspected to be polymer promoted and stabi lized LCP, a 1D NMR spectrum of the system at the condition indicated with a circle in Fig. 8 was obtained and is shown in Fig. 10 and 11. The effect of apparent PILP formation severely distorts the spectral peak. As seen in Fig. 10, there is an emergent peak splitting from the bulk solution peak in the upfield direction, indicating that a significant fraction of the buffer is favoring bicarbonate as compared to the bulk solution over a large multisecond time average. Fig. 11 shows the time evolution of the two phase bulk solution PILP sample. The process required hours to develop but solid nucleation and precipitation did not occur as evidenced by the unchanging area of the peaks. Fig. 11 shows a 1D NMR spectral comparison after 18 h (to attempt to achieve equilibrium) of the one phase, pH 8.5, bicarbonate buffer and PAsp solution *versus* the multiphase bicarbonate PAsp Ca^{2+} solution at the 17th injection. The two phase system emergent peak (bulge of separation from bulk solu tion) is shifted more upfield and is much larger than the NMR evidence of LCP precursor phase in the absence of additive, suggesting that polymer is stabilizing and accumulating a bicarbonate biased ionic interaction, which fits the description of the LCP phase, within a second bulk solution (mother solution) phase.

We used the same parameters and techniques to measure the T_2 relaxation and diffusion properties of the PILP system as described above for the LCP system. The results are shown in Fig. 12. Raw data for the CPMG (control), PFG STE (control), CPMG (phase separated PILP solution), and PFG STE (phase separated PILP solution) are shown in Fig. S.7 S.10† of the supplementary information, respectively. As with the LCP NMR experiments, the diffusion values obtained for the suspected PILP phase are not being presented as the diffusion of the large droplets. We believe this is the effective diffusion of the ion solute species that collect into, and are in exchange with, the PILP phase droplets. The diffusion

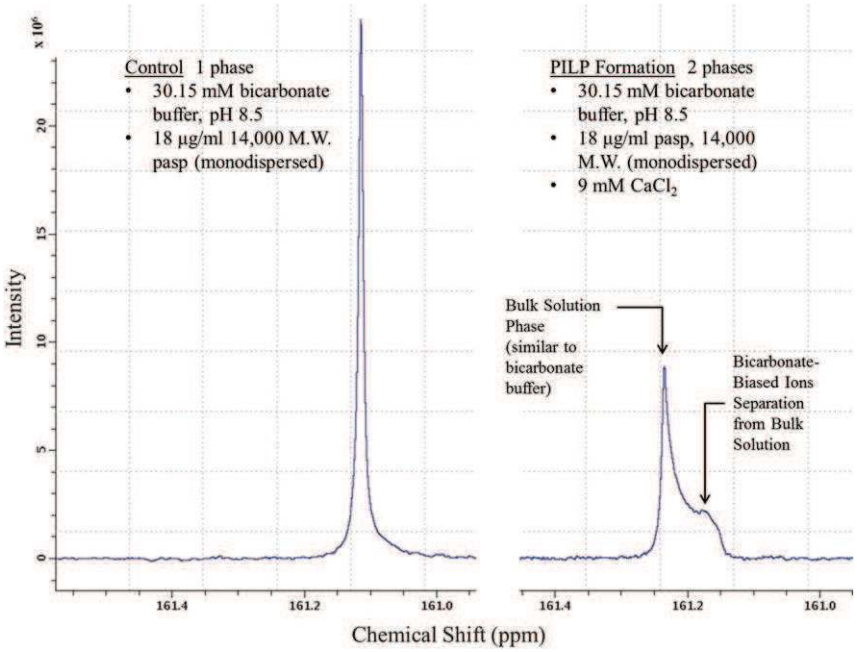

Fig. 10 A comparison between the 1D NMR spectra of bicarbonate buffer with polyaspartic acid sodium salt (left) and the separated bicarbonate biased ions (right). The presence of PAsp leads to a broad peak which is shifted upfield (bicarbonate weighted direction), distinct from the remaining ions in solution (bulk solution). This behavior is similar to the behavior of the liquid condensed phase except it is enhanced greatly in the presence of polymer, suggesting that the PILP process stabilizes the liquid condensed phase.

measurements were consistent in scale with those obtained for the LCP system. The presence of PAsp in the solution appeared to reduce the carbonate bicarbonate ion diffusion in general, but the ratios are similar to the LCP experiments and controls. The diffusion of phase separated ions (3×10^{-6} cm^2 s^{-1}) was a little less than half the diffusion of the carbonate bicarbonate in the bulk solution (7×10^{-6} cm^2 s^{-1}), and the bulk solution diffused at the same rate as the bicarbonate buffer control (both at 7×10^{-6} cm^2 s^{-1}). Using the Einstein Stokes equation, the effective diameter of the ionic species was 0.7 nm for the bulk solution and control carbonate bicarbonate ions, and was 1.6 nm for the bicarbonate biased ions. This is consistent with the slowed ions existing disproportionately as calcium monodentate/bidentate over this time average. Note the presence of the PAsp led to an overall slowing of the experimental and control diffusions, leading to the calculation of a larger effective diameter. This may be due to increased viscosity caused by the presence of the poly mer. Still, the ratio of diffusions (bicarbonate biased ion pairs : mother solu tion : control) were consistent with the non polymer case and demonstrate the separation of two distinct equilibria, which are comprised of ions diffusing at different rates. As explained for the non polymer case, this could be due to singular ions in a more viscous emergent PILP phase. If this were the case, the emergent PILP phase would have a viscosity of 0.02 dyne sec cm^2, according to the Einstein Stokes equation.

The T_2 relaxation of the upfield bulge was 1.1 msec, which suggests that the bicar bonate biased ions are slowly tumbling and rotating in solution. It was almost exactly the same as the bulk solution; both were shorter than the relaxation measured for the polymer bicarbonate buffer control (1.5 msec). Although a distinc tion between suspected PILP phase and the bulk solution would have been helpful in

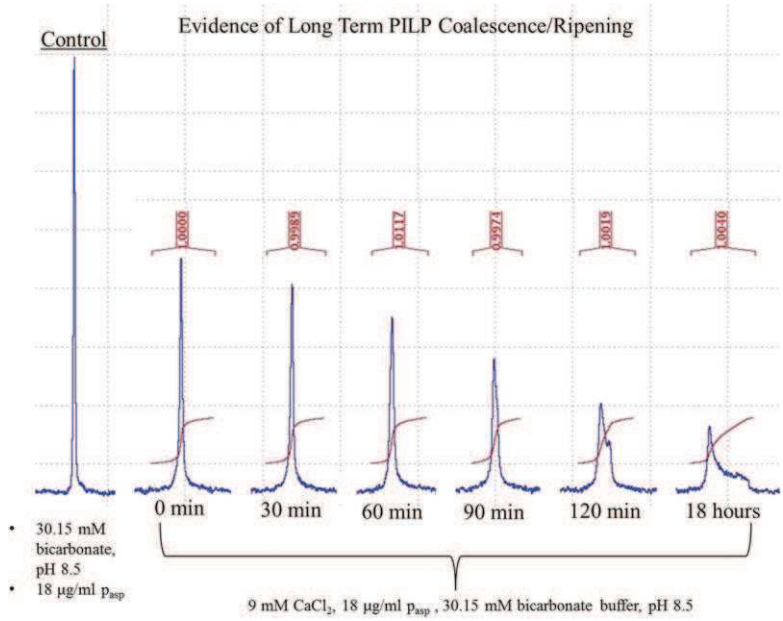

Fig. 11 The time evolution of a 1D NMR spectrum of the phase separated PILP containing solution shown in Fig. 10. Initially, it is broader than the control solution (absent of $CaCl_2$) as was observed for the formation of liquid condensed phase. However, in time a more distinct phase separation occurs to yield a large fraction of bicarbonate bias of the ions distinct from the bulk solution phase, suggesting the possibility of slow ripening and coalescence of LCP phase. The red, bracketed numbers above each spectral peak represent the area under the peak, normalized with respect to the 0 min spectrum. The amount of signal remains constant suggesting that all the ions are still behaving as solution state; therefore, solid nucleation and precipitation has not occurred.

distinguishing between types of phase environments, it is not surprising that they are similar due to the appearance of heavy chemical exchange between the them, as evi denced by the bridging between the suspected PILP peak and the mother solution peak (see Fig. 10).

As a side note, the spectrum of the separated PILP phase shown in Fig. 10 resem bles a powder pattern, which is an NMR spectral pattern obtained when there are solid particles present. However, a true powder pattern due to solids in solution would yield a broad spectrum peak with a width of 100 ppm. The width of the bulk solution PILP peak is only 0.1 ppm. This could mean that there is a slowing in the rotation of the bicarbonate carbonate ions but that the ion's rotations are still very rapid as expected for a solute in solution.

Discussion

The nucleation pathway of calcium carbonate through a multi step process, where the first step is the formation of a metastable liquid and the second is the solid nucle ation formation (within or outside the metastable liquid) has been at the forefront in recent literature.[3,34,52] Here, we have presented data that supports the first step of this assertion through a combination of techniques: in the absence of polymer additives, the ITC, Ca^{2+} binding profiles, and pH evolution experiments indicate that there is a phase transition. The pH measurements suggest the carbonate bicarbonate binding becomes bicarbonate biased, as do NMR peak emergences in the bicarbonate direc tion suggesting that bicarbonate is playing a role in the emergent phase. The fluidic

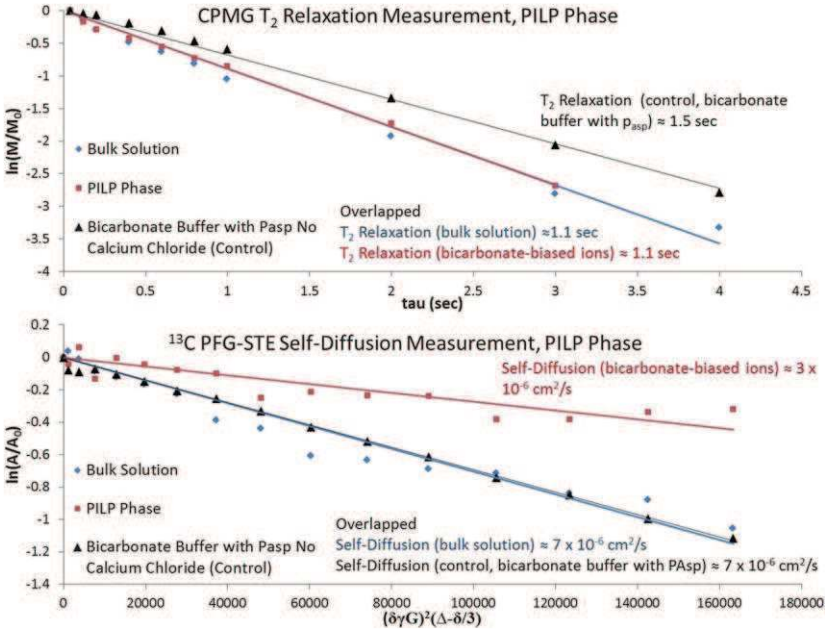

Fig. 12 The results of the CPMG T2 relaxation measurement (top) and the 13C PFG STE self diffusion measurement (bottom) of the PILP phase (suspected polymer stabilized LCP), bulk solution, and bicarbonate buffer with polyaspartic acid (control). The CPMG plot (top) is plotting the left side of equation 1 *vs.* the tau on the right side. The result is a linear relationship with a slope of $1/T_2$. The diffusion measurement plot (bottom) plots the left side of equation 2 *vs.* the right side where the slope of the resulting line is D (diffusion constant). The bicarbonate biased ions have the same T_2 relaxation as the bulk solution due to the large amount of chemical exchange, but have a shorter T_2 relaxation than the bicar bonate buffer control, suggesting that rotations of the bicarbonate biased ions are slowed. The diffusion of the bicarbonate biased ions is slowed with respect to the bulk solution and the bicarbonate buffer control in a way similar to LCP, suggesting that polymer is kinetically stabilizing the LCP phase.

character of this nucleated phase is suggested in the sedimentation properties of the species in solution and the apparent co existence of a distinct solution like liquid phase within the mother solution, as measured by AUC and NMR self diffusion and relaxation times, respectively.

Gebauer *et al.*[20] and Wolf *et al.*[45] claim that PNCs do not contain significant amounts of the bicarbonate ion. Computer simulations have suggested that DOLLOP PNCs are ubiquitous and exhibit incredibly quick dynamics on the order of picoseconds and nanoseconds.[22] For these reasons, we believe that the nucleation phenomenon we are seeing cannot be described by PNC theory. The apparent bicar bonate biased constituents we detect accompanying the precursor phase manifest their properties for long enough lifetimes to detect, suggesting that the LCP precursor phase is not forming from carbonate rich PNCs. We propose that in the LCP phase, there is a bicarbonate biased Ca^{2+} interaction which is distinct from the Ca^{2+} interaction with carbonates bicarbonate in the bulk solution over significant time averages. The presence of Ca bicarbonate ion pairing phenomenon or even clustering does not challenge the validity of predominantly Ca carbonate PNCs, like DOLLOP. These two phenomena are not mutually exclusive. At high pHs it is expected that the numerous CO_3^{2} ions, with their greater binding affinity to Ca^{2+} would dominate. However, at more neutral pHs, like the pH in which this study was conducted, there are relatively few CO_3^{2} ions as compared to HCO_3 ions and weaker Ca bicarbonate ion pairing or clustering phenomenon become

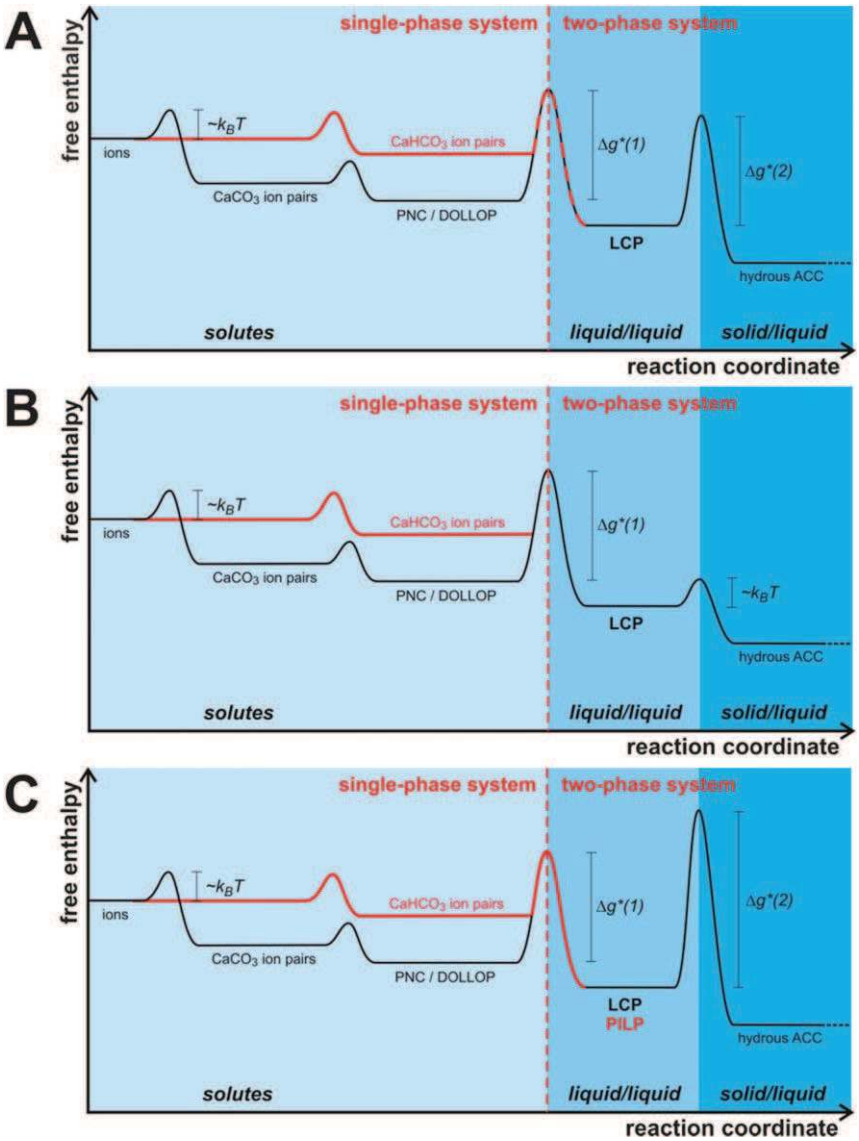

Fig. 13 An overview of the energetics (not to scale) of calcium carbonate precipitation from supersaturated solution, putting LCP into a global context with earlier findings. The diagram has been truncated on the right where the hydrous ACC will ultimately transform into a more stable crystalline phase. In solution, calcium bicarbonate and calcium carbonate ion pairs form, the latter of which can associate into larger species, PNCs including dynamically ordered, liquid like oxyanion polymers (DOLLOP). The different prenucleation species form virtually spontaneously (thermal energy k_BT), while formation of LCP is associated to a barrier of nucle ation $\Delta g^*(1)$. (A) At neutral pHs, the nucleation step involves calcium bicarbonate species, and with it, leads to a bicarbonate bias in the LCP and an intrinsic kinetic stabilization, $\Delta g^*(2)$, (B) At higher pH levels, calcium bicarbonate ion pairing becomes negligible, carbonate species dominate the nucleation process, and render LCP transient due to a reduced intrinsic stabiliza tion. The barrier $\Delta g^*(2)$, may even vanish. (C) Addition of PAsp may lead to a distinct increase of the barrier $\Delta g^*(2)$ due to a pronounced role of bicarbonate species in the LCP in the presence of polymer. The bicarbonate pathway may be preferred in the presence of polymer, and/or the polymer may stabilize bicarbonate species within LCP.

significant, leading to accumulation and nucleation of a bicarbonate rich metastable liquid phase like the one that has been proposed in this study.

This is significant because it has been proposed that nucleation of solid $CaCO_3$ can occur through nucleation inside of a metastable liquid phase.[53] The seed nucleus is proposed to form within the droplet and its growth and polymorph is subject to the environment of the metastable droplet, rather than that of the bulk solution. If metastable droplets of bicarbonate biased Ca^{2+} interactions phase separate and are stabilized by the presence of polymer (PILP process), as is possible with the drop lets observed in this study, then this might explain the incredible amount of nucle ation inhibition that polymers (particularly negatively charged, aspartic and glutamic acid rich polymers) give to a solution. An emergent metastable bicarbonate droplet and its smaller constituents would sequester Ca^{2+} and carbonate bicar bonate ions from the solution, thus mitigating the solid phase nucleation through PNC non classical pathways. However, the resulting concentrated metastable droplet would have difficulty forming a seed nucleation because it is bicarbonate biased and would require the extra step of releasing the H^+ ions prior to organization into a nucleus. We propose that LCP and PILP (PAsp stabilized LCP) plays a role in the calcium carbonate energetic cascade from supersaturated solution to crystallinity as described in Fig. 13.

Knowing what the PILP phase is may provide insight into various biological sys tem's mechanism of control over morphology, phase, and location of the final biomineral products. Although the presence of PNCs and LCP are interesting with respect to theoretical models of crystallization mechanisms, without the poly mer, the final products simply resemble those predicted by classical models. It is the accumulating and stabilizing effect of the polymer that allows for manipulation of the liquid condensed phase into an endless array of non equilibrium morphol ogies. On the other hand, without this propensity of the mineral reactants to form this liquid condensed phase, it is not clear that the polymer would be able to "induce" a liquid precursor phase. This work shows the significance of both sides of this interesting mineralization system.

Acknowledgements

We thank the Deutsche Forschungsgemeinschaft and National Science Foundation for financial support of this project within the "Materials World Network to Study Liquid Precursor Formation and Crystallization at Interfaces: Fundamentals towards Applications" (NSF Grant DMR 0710605 and DFG Grant CO 194/5 1, VO 829/4 1). Dirk Haffke (Konstanz) is acknowledged for NTA analysis, Rose Rosenberg, Dirk Haffke and Antje Völkel (Konstanz) for AUC experiments.

References

1 H. A. Lowenstam and S. Weiner, *On Biomineralization*, Oxford University Press, N. Y., 1989.
2 S. Mann, J. Webb and R. J. P. Williams, *Biomineralization: Chemical and Biochemical Perspectives*, VCH Publishers Inc., N. Y., 1989.
3 L. B. Gower, *Chem. Rev.*, 2008, **108**, 4551 4627.
4 F. C. Meldrum and H. Coelfen, *Chem. Rev.*, 2008, **108**, 4332 4432.
5 S. W. Lee, S. B. Park, S. K. Jeong, K. S. Lim, S. H. Lee and M. C. Trachtenberg, *Micron*, 2010, **41**, 273 282.
6 Y. Zhao, Y. Lu, Y. Hu, J. P. Li, L. Dong, L. N. Lin and S. H. Yu, *Small*, 2010, **6**, 2436 2442.
7 S. Biradar, P. Ravichandran, R. Gopikrishnan, V. Goornavar, J. C. Hall, V. Ramesh, S. Baluchamy, R. B. Jeffers and G. T. Ramesh, *J. Nanosci. Nanotechnol.*, 2011, **11**, 6868 6874.
8 J. Seto, Y. Ma, S. A. Davis, F. Meldrum, A. Gourrier, Y. Y. Kim, U. Schilde, M. Sztucki, M. Burghammer, S. Maltsev, C. Jager and H. Colfen, *Proc. Natl. Acad. Sci. U. S. A.*, 2012, **109**, 3699 3704.

9 I. Sethmann and G. Woerheide, *Micron*, 2008, **39**, 209 228.
10 D. Ren, Z. Li, Y. Gao and Q. Feng, *Biomed. Mater.*, 2010, **5**, 055009.
11 E. Beniash, L. Addadi and S. Weiner, *J. Struct. Biol.*, 1999, **125**, 50 62.
12 N. Gehrke, N. Nassif, N. Pinna, M. Antonietti, H. S. Gupta and H. Colfen, *Chem. Mater.*, 2005, **17**, 6514 6516.
13 F. C. Meldrum, *Int. Mater. Rev.*, 2003, **48**, 187 224.
14 J. Rieger, T. Frechen, G. Cox, W. Heckmann, C. Schmidt and J. Thieme, *Faraday Discuss.*, 2007, **136**, 265 277.
15 J. Aizenberg, *Bell Labs Tech. J.*, 2005, **10**, 129 141.
16 P. Fratzl, F. D. Fischer, J. Svoboda and J. Aizenberg, *Acta Biomater.*, 2010, **6**, 1001 1005.
17 L. B. Gower and D. J. Odom, *J. Cryst. Growth*, 2000, **210**, 719 734.
18 B. Guillemet, M. Faatz, F. Grohn, G. Wegner and Y. Gnanou, *Langmuir*, 2006, **22**, 1875 1879.
19 D. Gebauer and H. Colfen, *Nano Today*, 2012, **6**, 564 584.
20 D. Gebauer, A. Volkel and H. Colfen, *Science*, 2008, **322**, 1819 1822.
21 E. M. Pouget, P. H. H. Bomans, J. Goos, P. M. Frederik, G. de With and N. Sommerdijk, *Science*, 2009, **323**, 1455 1458.
22 R. Demichelis, P. Raiteri, J. D. Gale, D. Quigley and D. Gebauer, *Nat. Commun.*, 2011, **2**, 590.
23 J. Rieger, T. Frechen, G. Cox, W. Heckmann, C. Schmidt and J. Thieme, *Faraday Discuss.*, 2007, **136**, 265 277.
24 M. Faatz, F. Grohn and G. Wegner, *Adv. Mater.*, 2004, **16**, 996.
25 S. E. Wolf, L. Mueller, R. Barrea, C. J. Kampf, J. Leiterer, U. Panne, T. Hoffmann, F. Emmerling and W. Tremel, *Nanoscale*, 2011, **3**, 1158 1165.
26 S. J. Homeijer, R. A. Barrett and L. B. Gower, *Cryst. Growth Des.*, 2010, **10**, 1040 1052.
27 S. J. Homeijer, M. J. Olszta, R. A. Barrett and L. B. Gower, *J. Cryst. Growth*, 2008, **310**, 2938 2945.
28 F. F. Amos, L. Dai, R. Kumar, S. R. Khan and L. B. Gower, *Urol. Res.*, 2009, **37**, 11 17.
29 A. Dey, P. H. H. Bomans, F. A. Mueller, J. Will, P. M. Frederik, G. de With and N. A. J. M. Sommerdijk, *Nat. Mater.*, 2010, **9**, 1010 1014.
30 S. S. Jee, R. K. Kasinath, E. DiMasi, Y. Y. Kim and L. Gower, *CrystEngComm*, 2011, **13**, 2077 2083.
31 S. S. Jee, T. T. Thula and L. B. Gower, *Acta Biomater.*, 2010, **6**, 3676 3686.
32 T. T. Thula, D. E. Rodriguez, M. H. Lee, L. Pendi, J. Podschun and L. B. Gower, *Acta Biomater.*, 2011, **7**, 3158 3169.
33 S. S. Jee, L. Culver, Y. Li, E. P. Douglas and L. B. Gower, *J. Cryst. Growth*, 2010, **312**, 1249 1256.
34 P. G. Vekilov, *Cryst. Growth Des.*, 2010, **10**, 5007 5019.
35 O. Galkin, W. Pan, L. Filobelo, R. E. Hirsch, R. L. Nagel and P. G. Vekilov, *Biophys. J.*, 2007, **93**, 902 913.
36 Y. Jiang, H. Gong, D. Volkmer, L. Gower and H. Coelfen, *Adv. Mater.*, 2011, **23**, 3548.
37 Y. Jiang, L. Gower, D. Volkmer and H. Colfen, *Phys. Chem. Chem. Phys.*, 2012, **14**, 914 919.
38 Y. Jiang, L. Gower, D. Volkmer and H. Colfen, *Cryst. Growth Des.*, 2011, **11**, 3243 3249.
39 S. Wohlrab, H. Colfen and M. Antonietti, *Angew. Chem., Int. Ed.*, 2005, **44**, 4087 4092.
40 Y. Ma, G. Mehltretter, C. Plueg, N. Rademacher, M. U. Schmidt and H. Coelfen, *Adv. Funct. Mater.*, 2009, **19**, 2095 2101.
41 A. V. Radha, T. Z. Forbes, C. E. Killian, P. U. P. A. Gilbert and A. Navrotsky, *Proceedings of the National Academy of Sciences*, 2010, **107**, 16438 16433.
42 D. Gebauer, A. Verch, H. G. Boerner and H. Coelfen, *Cryst. Growth Des.*, 2009, **9**, 2398 2403.
43 P. Schuck, *Biophys. J.*, 2000, **78**, 1606 1619.
44 P. Schuck, *Biophys. J.*, 1998, **75**, 1503 1512.
45 S. E. W. S. E. Wolf, L. Muller, R. Barrea, C. J. Kampf, J. Leiterer, U. Panne, T. Hoffmann, F. Emmerling and W. Tremel, *Nanoscale*, 2011, **3**, 1158 1165.
46 K. Strenge and A. Seifert, *Prog. Colloid Polym. Sci.*, 1991, **86**, 76 83.
47 H. Nebel, M. Neumann, C. Mayer and M. Epple, *Inorg. Chem.*, 2008, **47**, 7874 7879.
48 F. M. Michel, J. MacDonald, J. Feng, B. L. Phillips, L. Ehm, C. Tarabrella, J. B. Parise and R. J. Reeder, *Chem. Mater.*, 2008, **20**, 4720 4728.
49 R. E. Zeebe, *Geochim. Cosmochim. Acta*, 2011, **75**, 2483 2498.
50 K. Kigoshi and T. Hashitani, *Bull. Chem. Soc. Jpn.*, 1963, **36**, 1372 1372.
51 A. Verch, D. Gebauer, M. Antonietti and H. Colfen, *Phys. Chem. Chem. Phys.*, 2011, **13**, 16811 16820.
52 D. Gebauer and H. Coelfen, *Nano Today*, 2011, **6**, 564 584.
53 P. G. Vekilov, *Cryst. Growth Des.*, 2004, **4**, 671 685.